

Enhanced electroluminescence intensity of InGaN/GaN multi-quantum-wells based on Mg-doped GaN annealed in O₂

Ping Ma, Yanqin Gai,^{a)} Junxi Wang, Fuhua Yang, Yiping Zeng, Jinmin Li, and Jingbo Li^{b)}

International Cooperation Base for Solid State Lighting, Institute of Semiconductors, Chinese Academy of Sciences, P.O. Box 912, Beijing 100083, China

(Received 4 August 2008; accepted 11 August 2008; published online 11 September 2008)

InGaN/GaN multi-quantum-well blue (461 ± 4 nm) light emitting diodes with higher electroluminescence intensity are obtained by postgrowth thermal annealing at 720 °C in O₂-ambient. Based on our first-principle total-energy calculations, we conclude that besides dissociating the Mg–H complex by forming H₂O, annealing in O₂ has another *positive* effect on the activation of acceptor Mg in GaN. Mg can be *further* activated by the formation of an impurity band above the valence band maximum of host GaN from the passivated Mg_{Ga}–O_N complex. Our calculated ionization energy for acceptor Mg in the passivated system is about 30 meV shallower than that in pure GaN, in good agreement with previous experimental measurement. Our model can explain that the enhanced electroluminescence intensity of InGaN/GaN MQWs based on Mg-doped *p*-type GaN is due to a decrease in the ionization energy of Mg acceptor with the presence of oxygen. © 2008 American Institute of Physics. [DOI: 10.1063/1.2980032]

Large ionization energy of the preferred acceptor Mg in GaN ranging from 160 to 200 meV renders that there is only about 1% of Mg is activated at room temperature.^{1–4} Such carrier concentration is well below that for device application ($\geq 10^{17}$ cm⁻³). In order to obtain higher external quantum efficiency of GaN-based blue light emitting diodes (LEDs), improvement in *p*-type conductivity control of GaN film is one of the urgent requirements. Recently, deliberate incorporation of donor oxygen in Mg-doped GaN is one successful method to improve the conductivity of *p*-type GaN.^{5,6} Hole concentration approaching 2×10^{17} cm⁻³ can be achieved by Mg codoped with oxygen. It is believed that the higher hole concentration of the (Mg, O)-codoped GaN is due to the enhanced Mg solubility and the decreased ionization of acceptor Mg with the addition of oxygen. Kipshidze *et al.*⁶ ascribed the reduction in the ionization energy to the potential interactions between free hole and the ionized acceptor.⁷ Several groups *even* proved that the presence of oxygen in the postgrowth thermal annealing environment exhibits strong influence on the activation of Mg in GaN. Koide *et al.*⁸ recently demonstrated that annealed in O₂ containing ambient at 500–600 °C results in improved Ohmic contact and lower sheet resistance of the semiconductor. Hull *et al.*⁹ annealed the Mg-doped GaN sample in four gas mixtures containing different percentages of O₂, respectively, and found that the resistivity of the *p*-type GaN was greatly reduced in the presence of O₂, where they *all* attribute the activation of Mg to the removal of residual hydrogen from the *p*-type GaN to form H₂O at the GaN surface.

In this letter, based on InGaN/GaN multi-quantum-well (MQW) blue LED postgrowth thermal annealing experiments and first-principle total-energy calculations, we propose that Mg-doped *p*-type GaN can be *further* activated by the formation of an impurity band from the passivated Mg_{Ga}–O_N complex above the valence band maximum (VB-

M)of host GaN if the sample is thermally treated in O₂-ambient after growth or is intentionally codoped with oxygen, as indicated in Fig. 1. The calculated ionization energy of Mg_{Ga} in the newly formed system is about 30 meV shallower than that in pure GaN, which agrees well with the (Mg, O)-codoping experiment.⁵

The first-principle total-energy calculations in this study are performed using the density functional theory in the local density approximation as implemented in the plane wave VASP code.¹⁰ The electron and core interactions are described using the frozen-core projected augmented wave methods.¹¹ The Ga 3*d* electrons are explicitly treated as valence states. The wave function is expanded in plane waves with a cutoff energy of 400 eV. The Brillouin zone integrations for charge density and total-energy calculations are performed using the *k*-points that are equivalent to the $4 \times 4 \times 4$ Monkhorst-Pack¹² special *k*-point meshes in the zinc-blende (ZB) Brillouin zone. For all the doped system, a $2 \times 2 \times 2$ supercell constructed from the ZB GaN unit cell is employed. The lattice constants of the supercell are kept fixed to those of pure GaN and all the internal parameters are allowed

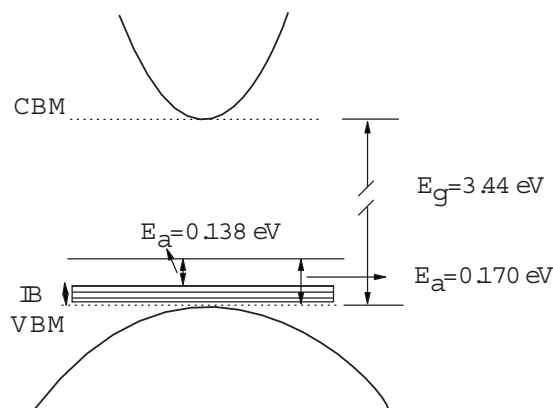


FIG. 1. The schematic plot for the ionization of acceptor Mg in the presence of an impurity band above the VBM of GaN.

^{a)}Electronic mail: yqgai@semi.ac.cn.

^{b)}Electronic mail: jbli@semi.ac.cn.

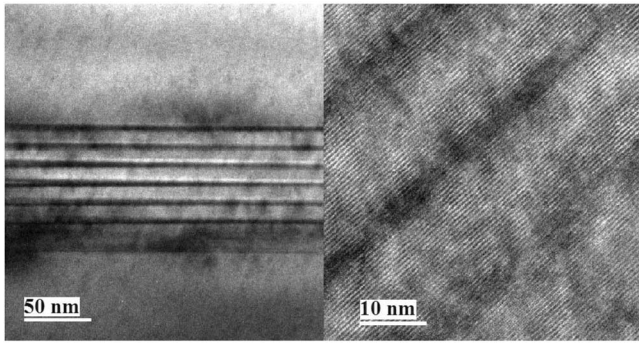


FIG. 2. High-resolution TEM images with different magnifications of the InGaN/GaN MQWs.

to relax until the Hellmann–Feynman forces acting on the atoms become less than $0.01 \text{ eV}/\text{\AA}$.

The ionization energy of an isolated acceptor α with respect to the VBM is calculated following the conventional procedure described in (Ref. 13),

$$\varepsilon(0/q) = \{E(\alpha, q) - [E(\alpha, 0) - q\varepsilon_D^k] / (-q) + [\varepsilon_D^\Gamma - \varepsilon_{\text{VBM}}^\Gamma(\text{host})]\} / (-q) \quad (q < 0), \quad (1)$$

where, $E(\alpha, q)$ and $E(\alpha, 0)$ are the total energies of the supercell in charge state q and neutral for impurity α calculated using the special k -points. $\varepsilon_D^k(0)$ and $\varepsilon_D^\Gamma(0)$ are the defect level at the special k -points (averaged) and at Γ -point, respectively. $\varepsilon_{\text{VBM}}^\Gamma(\text{host})$ is the VBM energy of host supercell at Γ -point and E_F is the Fermi level with respect to the VBM. The second term on the right hand side of Eq. (1) is the single particle energy level at Γ -point and is aligned using core electron energy levels away from the defects.

Our InGaN/GaN MQW blue LED samples were grown on c -plane (0001) sapphire substrate by metal-organic chemical vapor deposition (MOCVD) method. Ammonia (NH_3), trimethyl-gallium (TMGa), trimethylindium (TMIn), biscyclopentadienilmagnesium (Cp_2Mg), and silane (SiH_4) were used as precursors and dopants. The substrates were initially treated in H_2 at 1080°C followed by a 25-nm-thick low-temperature GaN buffer layer grown at 525°C . After a high-temperature annealing, a $2\text{-}\mu\text{m}$ -thick n -GaN layer was deposited at a temperature of 1050°C . The InGaN/GaN MQWs were subsequently grown at a low temperature of 750°C , consisting of eight periods of 10 nm GaN barriers and 3 nm InGaN wells. Above that, a 20-nm-thick $p\text{-Al}_{0.15}\text{Ga}_{0.85}\text{N}$ blocking layer and a 200-nm-thick p -GaN layer were deposited at 980°C , successively. After the growth, thermal treatments at 720°C were performed for the MQWs with 100-nm-, 150-nm-thick p -type layer in pure N_2 , $\text{N}_2/\text{O}_2=7/3$, $\text{N}_2/\text{O}_2=5/5$ and pure O_2 atmosphere, respectively. After thermal treatment, each sample was examined by electroluminescence (EL) measurements at a forward current of 20 mA and at room temperature. High quality of InGaN/GaN MQWs is confirmed by cross-sectional transmission electron microscopy (TEM) images, as shown in Fig. 2.

Figure 3 shows the 20 mA EL spectra comparison of the LEDs with different thicknesses of p -type GaN layer as-grown and after treated in N_2 . It can be seen from Fig. 3 that the EL intensity of the activated samples is increased than the unannealed ones. This is because that N_2 -ambient ther-

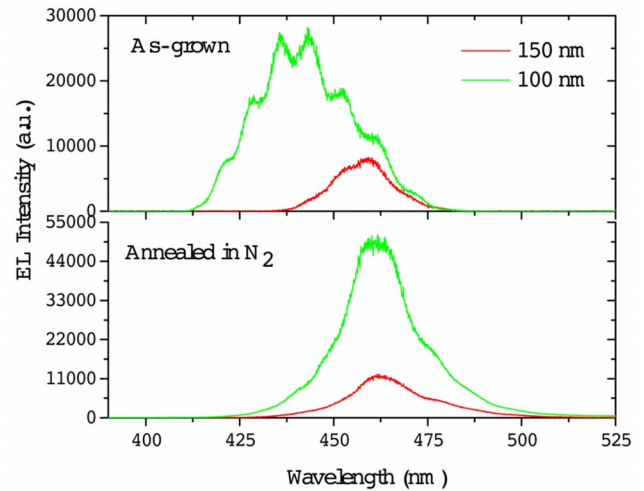


FIG. 3. (Color online) The EL spectra of blue InGaN LEDs at a forward current of 20 mA with different thicknesses of p -type GaN before and after annealed in N_2 .

mal annealing at temperatures above 700°C can remove atomic hydrogen from the Mg–H neutral complex, and the resistivity of p -type GaN films becomes lower after this annealing process. The peak wavelength of the treated samples are located at $461 \pm 4 \text{ nm}$, indicating blue EL.¹⁴ For the samples with 150-nm-thick p -type layer, such treatment does not improve the EL intensity apparently, this is because that these Mg-doped GaN films are too thick that the amount of penetrated oxygen is not large enough to lead to the formation of the impurity band. Therefore, in order to activate the Mg acceptor as large magnitude as possible, proper thickness of the p -type layer must be carefully chosen during the device fabrication considering the crystal quality and p -type conductivity. To investigate the effect of oxygen on the reactivation of acceptor Mg, the room temperature EL spectra of the samples annealed in gas mixture with different percentages of O_2 content are measured at a forward current of 20 mA and are given in Fig. 4. We can see from Fig. 4 that the magnitude of the EL signal is strongly enhanced with the increase in O_2 content in the annealing environment. Such a

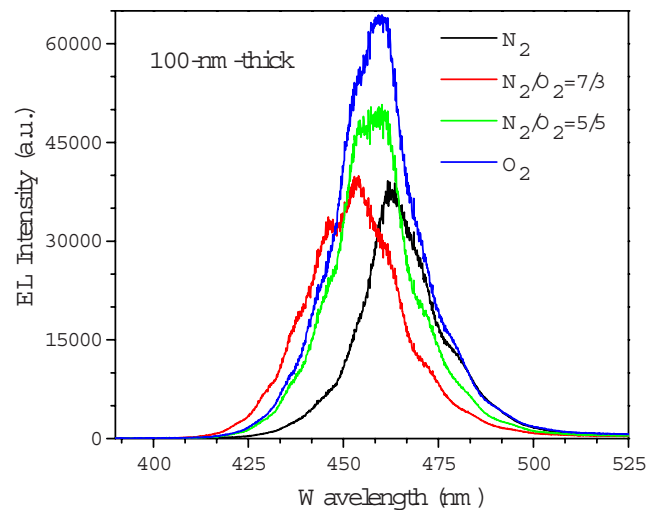


FIG. 4. (Color online) The EL spectra of blue InGaN LED with a 100-nm-thick p -type layer annealed in different ambients measured at a forward current of 20 mA.

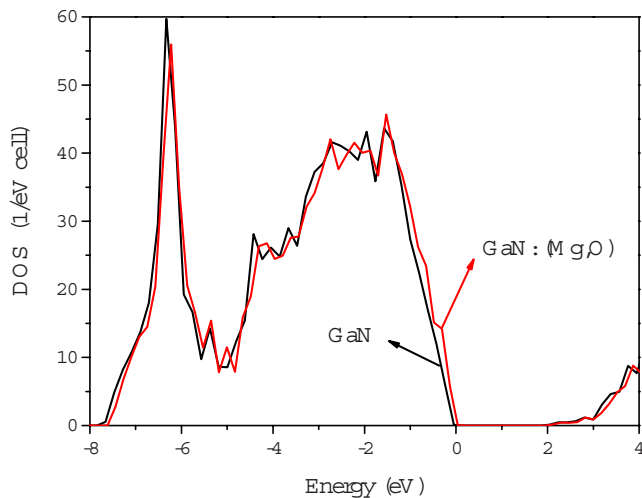


FIG. 5. (Color online) Calculated total DOS for supercells of pure GaN, and GaN containing passivated (Mg, O) complexes.

significant increase in EL intensity can be attributed to the availability of significantly increased hole concentration in the *p*-type GaN. Of course, we do not deny the other effect of oxygen during thermal annealing, such as the outdiffusion of hydrogen by forming H_2O , especially for samples grown by MOCVD method.^{15–17} Based on our calculations, acceptor Mg_{Ga} can be further activated with the existence of oxygen in the sample.

To explain the results obtained above, the total density of states (DOS) for pure GaN and GaN containing the passivated $Mg_{Ga}-O_N$ complexes are given in Fig. 5. The formation of a donor-acceptor complex is the precondition in our model, the calculated binding energy for the $Mg_{Ga}-O_N$ complex is 3.59 eV (a positive binding energy means a stable complex). The mutual passivated complex does not offer carriers, but forming an additional band just above the VBM of host, as indicated by the DOS curve in Fig. 5. With the formation of such impurity band, the excessive acceptor is now activated by electrons from the impurity band maximum (IBM) rather than from the VBM of GaN.¹⁸ Our model proposed here proved that the postgrowth annealing in O_2 has another effect on the activation of acceptor Mg, and clarify the exact physical mechanism responsible for the realization of high conductivity *p*-type GaN by Mg codoped with oxygen.

In summary, the EL spectra of the InGaN/GaN MQW blue LEDs with different thicknesses of *p*-type layers post-

growth thermally treated in different gas ambients are measured. We find that the EL intensity is greatly enhanced when the sample with a 100-nm-thick Mg-doped GaN is annealed in O_2 . We have calculated the ionization energies of acceptor Mg in pure GaN and in (Mg, O) passivated GaN by first-principles total-energy calculations. Our results suggest that it is the formation of the fully occupied impurity band above the VBM of host GaN arising from the passivated $Mg_{Ga}-O_N$ complex that renders the acceptor Mg_{Ga} shallower at about 0.138 eV above the IBM. This model can explain that the enhanced EL intensity of quantum device based on Mg-doped *p*-type GaN is due to the reactivation of Mg acceptor through postgrowth annealing in O_2 , besides the dissociation of Mg-H complex by forming H_2O .

J.L. gratefully acknowledges financial support from the “One-Hundred Talents Plan” of the Chinese Academy of Sciences. This work was supported by the National Natural Science Foundation of China and the National High Technology Research and Development program of China under Contract No. 2006AA03A22.

- ¹T. Tanaka, A. Watanabe, H. Amano, Y. Kobayashi, and I. Akasaki, *Appl. Phys. Lett.* **65**, 593 (1994).
- ²W. Götz, N. M. Jonson, J. Walker, D. P. Bour, and R. A. Street, *Appl. Phys. Lett.* **68**, 667 (1996).
- ³W. Kim, A. Salvador, A. E. Botchkarev, O. Aktas, S. N. Mahammad, and H. Morkoç, *Appl. Phys. Lett.* **69**, 559 (1996).
- ⁴W. Kim, A. E. Botchkarev, A. Salvador, G. Popovici, H. Tang, and H. Morkoç, *Appl. Phys. Lett.* **82**, 219 (1997).
- ⁵R. Y. Korotkov, J. M. Gregie, and B. W. Wessels, *Appl. Phys. Lett.* **78**, 222 (2001).
- ⁶G. Kipshidze, V. Kuryatkov, B. Borisov, Yu. Kudryavtsev, R. Asomoza, S. Nikishin, and H. Temkin, *Appl. Phys. Lett.* **80**, 2910 (2002).
- ⁷H. Reiss, C. S. Fuller, and F. J. Morin, *Bell Syst. Tech. J.* **35**, 535 (1956).
- ⁸Y. Koide, T. Maeda, T. Kawakami, S. Fujita, T. Uemura, N. Shibata, and M. Murakami, *J. Electron. Mater.* **28**, 341 (1999).
- ⁹B. A. Hull, S. E. Mohny, H. S. Venugopalan, and J. C. Ramer, *Appl. Phys. Lett.* **76**, 2271 (2000).
- ¹⁰G. Kresse and J. Hafner, *Phys. Rev. B* **47**, R558 (1993); **48**, 13115 (1993).
- ¹¹P. E. Blöchl, *Phys. Rev. B* **50**, 17953 (1994); G. Kresse and J. Joubert, *ibid.* **59**, 1758 (1999).
- ¹²H. J. Monkhorst, and J. D. Pack, *Phys. Rev. B* **16**, 1748 (1977).
- ¹³S.-H. Wei, *Comput. Mater. Sci.* **30**, 337 (2004).
- ¹⁴H. Amano and I. Akasaki, *Oyo Butsuri* **60**, 163 (1991) (in Japanese).
- ¹⁵W. Seifert, R. Franzheld, E. Butter, H. Sobotta, and V. Riede, *Cryst. Res. Technol.* **18**, 383 (1983).
- ¹⁶B.-C. Chung and M. Gershenson, *J. Appl. Phys.* **72**, 651 (1992).
- ¹⁷T. Yamamoto and H. Katayama-Yoshida, *Jpn. J. Appl. Phys., Part 2* **36**, L180 (1997).
- ¹⁸Y. Yan, J. Li, S.-H. Wei, and M. M. Al-Jassim, *Phys. Rev. Lett.* **98**, 135506 (2007).